Acta Mechatronica - International Scientific Journal about Mechatronics
Volume: 7 2022 Issue: 1 Pages: 1-7 ISSN 2453-7306

doi:10.22306/am.v7i1.82

Received: 03 Feb. 2022
Revised: 18 Feb. 2022
Accepted: 02 Mar. 2022

Kinematic motion analysis of the members of a double jaw crusher

Darina Hroncova
Department of Mechatronics, Faculty of Mechanical Engineering, Technical University of Košice, Park Komenského 8, 042 00 Košice, Slovak Republic, EU, darina.hroncova@tuke.sk (corresponding author)
Ingrid Delyova
Department of Applied Mechanics and Mechanical Engineering, Faculty of Mechanical Engineering, Technical University of Košice, Letná 9, 042 00 Košice, Slovak Republic, EU, ingrid.delyova@tuke.sk
Peter Frankovsky
Department of Applied Mechanics and Mechanical Engineering, Faculty of Mechanical Engineering, Technical University of Košice, Letná 9, 042 00 Košice, Slovak Republic, EU, peter.frankovsky@tuke.sk
Vojtech Neumann
Department of Applied Mechanics and Mechanical Engineering, Faculty of Mechanical Engineering, Technical University of Košice, Letná 9, 042 00 Košice, 042 00 Košice, Slovak Republic, EU, peter.frankovsky@tuke.sk
Dalibor Cech
Department of Applied Mechanics and Mechanical Engineering, Faculty of Mechanical Engineering, Technical University of Košice, Park Komenského 8, 042 00 Košice, Slovak Republic, EU, dalibor.cech@tuke.sk

Keywords: kinematic analysis, mechanism, simultaneous motion, simulation.
Abstract: Computational technology makes it possible to accelerate and simplify the processes of kinematic and dynamic analysis. The paper deals with the problem of kinematic analysis of a planar six-joint mechanism of a jaw double-spring crusher. Computational techniques and software support have been used in the kinematic analysis. The obtained results are compared with the results of the graphical solution. The graphical solution has been carried out by using CAD software. MSC.Adams/View program was used to create a model and simulate the jaw crusher motion. In both cases there was agreement of the obtained results.

1 Introduction

The development of computer technology has made it possible to simplify and speed up various processes in different industries. One of these industries is engineering. Computing is nowadays quite used in this field, it can be said that almost in the whole process of design, construction and production of a machine component, mechanism and others. The software that has been developed to facilitate the work of people in technical practice allows a given machine part to be designed as a 3D model, to combine multiple parts into an assembly to create a functional 3D model of, for example, a mechanism, to perform static, kinematic or dynamic analyses of parts, mechanisms, they also allow to plot the stresses of the parts, to simulate not only the processes of designing the parts, but also the simulation of the production of these parts. Last but not least, they save time and money because the designs can be carried out much faster compared to analytical methods, they also save the consumption of materials because they can simulate a number of things and processes in which it is possible to detect possible defects and shortcomings of a given component, mechanical system or manufacturing process before the prototype is made or production is started [1-3].

The aim of this thesis is to model the mechanism of a crusher with two struts in the MSC.Adams program environment, and then also to perform a kinematic analysis of the mechanism in this program.

2 Kinematic analysis of a double-spring crusher

The double jaw crusher is designed for crushing hard materials, also quarried materials, sand and gravel, and recycling. [4,5]

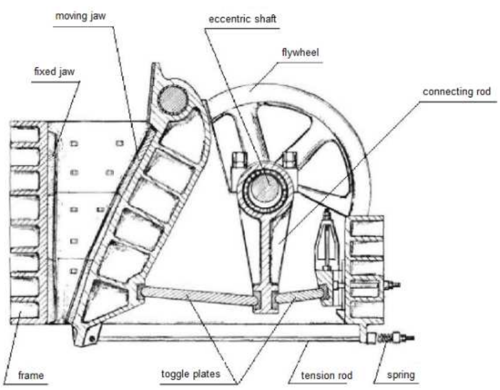

Figure 1 Description of the main parts of the double jaw crusher[4]

The tie rod and compression spring ensure that the buckling plates are in their bearings throughout the crusher run, and also assist in the reciprocating movement of the moving jaw. The kinematic analysis will be carried out on a simplified model of the crusher, where the rod and spring are neglected and the buckling plate fits are replaced by pivot joints. A simplified model (kinematic diagram) of the mechanism of the double buckling jaw crusher is shown in Fig. 20. The mechanism in question is a six membered mechanism formed by attaching a binary system group, composed of members 5 and 6, to a basic four membered crank mechanism composed of members 1, 2, 3 and 4. The members of this mechanism are a frame (1), an eccentric shaft, i.e. a crank (2), a connecting rod (3), a buckling plate, i.e. as it were a rocker arm (4), a second buckling plate (5) and a movable jaw with a pendulum (6) [4,5].

Member 2 is the driving member, the others are driven [6].

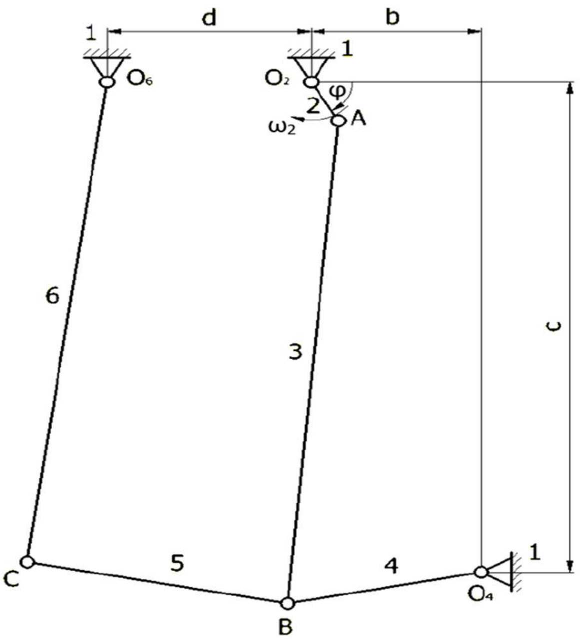

Figure 2 Kinematic diagram of the solved model - crusher mechanism

Every single moving member performs a planar motion, as it is a planar mechanism. Member 2 performs a uniform rotational motion about point O_2 with a constant angular velocity $\omega_2 = 6\pi\ rad/s$, the trajectory of point A is a circle. Members 4 and 6 also perform rotational motion, member 4 about point O_4 and member 6 about point O_6. The trajectories of points B and C are parts of a circle, namely circular arcs. Members 3 and 5 perform general planar motion. All these motions are related to the base space - the frame [6].

The dimensions of the individual members and the distances of the axes of rotation are: member 2 $O_2A = 40\ mm$, member 3 $AB = 430\ mm$, member 4 $O_4B = 145\ mm$, member 5 $BC = 195\ mm$, member 6 $O_6C = 430\ mm$, $b = 125\ mm$, $c = 435\ mm$, $d = 150\ mm$, uhol $\varphi = 60°$.

2.1 *Determining the velocity of individual members*

In the simultaneous motion of bodies, the resultant velocity of a given point or body consists of the drift velocity and the relative velocity, which can be determined graphically as a diagonal in a parallelogram, the sides of which are the vectors of the given velocity components. To determine the resultant velocity vector ($\boldsymbol{v}_v$), the vector summation relation of the drift velocity vector ($\boldsymbol{v}_u$) and the relative velocity vector ($\boldsymbol{v}_r$) holds [7]:

$$\boldsymbol{v}_v = \boldsymbol{v}_u + \boldsymbol{v}_r. \tag{1}$$

The magnitude of the velocity at point A can be determined by calculation at a known angular velocity.

$$v_{A21} = \omega_2 \overline{O_2A} = 0.75398\ m/s \tag{2}$$

When the motion of the members is decomposed, the velocity at point A is expressed by the equation.

$$\boldsymbol{v}_{A31} = \boldsymbol{v}_{A32} + \boldsymbol{v}_{A21} \tag{3}$$

Since point A is the common point of member 2 and member 3, the magnitude of the velocity $\boldsymbol{v}_{A32}$ is zero. Therefore, the velocity of point A is.

$$\boldsymbol{v}_{A31} = \boldsymbol{v}_{A21} = \boldsymbol{v}_A \tag{4}$$

Point B is a common point of Article 3 and Article 4 (also member 5). Thus, the magnitude of the velocity $\boldsymbol{v}_{B34}$ is zero. For the velocity at point B, with the decomposition of the motion $31 = 34 + 41$, the following is true.

$$\boldsymbol{v}_{B31} = \boldsymbol{v}_{B41} = \boldsymbol{v}_B \tag{5}$$

The velocity at point B can be determined graphically using the instantaneous centre of rotation of member 3 and the velocity at point A using the angle of view theorem. According to the decomposition of the motion, the vector equation holds for the velocity at point B.

$$\boldsymbol{v}_{B31} = \boldsymbol{v}_{A31} + \boldsymbol{v}_{BA31} \tag{6}$$

With respect to the reference point A, point B performs a planar rotational motion on a circle.

2.2 *Determining the accelerations of individual members*

Acceleration is generally a vector quantity that characterizes the temporal change in velocity of a point or body. When bodies move simultaneously, the resultant acceleration of a body or point is determined as the vector sum of the vector of the acceleration vector of the drift motion, the acceleration vector of the relative motion, and the Coriolis acceleration [7].

$$\boldsymbol{a}_v = \boldsymbol{a}_u + \boldsymbol{a}_r + \boldsymbol{a}_{cor}. \qquad (7)$$

For the Coriolis acceleration $\boldsymbol{a}_{cor}$, relation (8) is generally valid; it is the vector product of twice the angular velocity vector of the drift motion ($\boldsymbol{\omega}_u$) and the velocity vector of the relative motion ($\boldsymbol{v}_r$) [1].

$$\boldsymbol{a}_{cor} = 2\boldsymbol{\omega}_u \times \boldsymbol{v}_r \qquad (8)$$

The Coriolis acceleration is equal to zero when the translational drift is zero ($\boldsymbol{\omega}_u = 0$), or when the relative velocity at a given point is zero ($\boldsymbol{v}_r = 0$), or the vectors of these velocities are parallel at that point. When bodies are moving simultaneously in a plane, these vectors are perpendicular to each other, and thus the magnitude of the Coriolis acceleration is [7].

$$a_C = 2\omega_u v_r \qquad (9)$$

Point A is the common point of members 2 and 3, and hence the acceleration at this point is also.

$$\boldsymbol{a}_{A31} = \boldsymbol{a}_{A21} = \boldsymbol{a}_A \qquad (10)$$

Since member 2 rotates with a constant angular velocity ω_2, which results in a constant velocity v_A of point A, the acceleration of point A in the tangential direction is zero ($\boldsymbol{a}_{A21t} = 0\ ms^{-2}$). The acceleration at point A is equal to the normal component of the acceleration.

$$\boldsymbol{a}_{A21} = \boldsymbol{a}_{A21n} + \boldsymbol{a}_{A21t} \qquad (11)$$

$$\boldsymbol{a}_{A21} = \boldsymbol{a}_{A21n} \qquad (12)$$

The magnitude of the normal component of acceleration at a given point can be obtained using Euclidean construction.

It is known that point B is a common point of members 3 and 4 (and also of member 5), therefore.

$$\boldsymbol{a}_{B31} = \boldsymbol{a}_{B41} = \boldsymbol{a}_{B51} = \boldsymbol{a}_B \qquad (13)$$

The acceleration at point B will.

$$\boldsymbol{a}_{B31} = \boldsymbol{a}_{A31} + \boldsymbol{a}_{BA31} \qquad (14)$$

After decomposing the accelerations into tangential and normal components, relation (14) can be written in the form.

$$\boldsymbol{a}_{B31} = \boldsymbol{a}_{A31n} + \boldsymbol{a}_{A31t} + \boldsymbol{a}_{BA31n} + \boldsymbol{a}_{BA31t} \qquad (15)$$

From the solution of the acceleration at point A, it is known that the magnitude of the tangential component of the acceleration $\boldsymbol{a}_{A31t}$ at point A is equal to zero, and the normal component of this acceleration $\boldsymbol{a}_{A31n}$ is also known, the acceleration $\boldsymbol{a}_{A31}$ is known completely. The other accelerations in relation (15) are unknown and need to be determined. The individual magnitudes of the components of the accelerations of point B with respect to the overlap and of point B with respect to point A have been determined graphically and their values are given in Table 1.

Point C is the common point of members 5 and 6, therefore.

$$\boldsymbol{a}_{C51} = \boldsymbol{a}_{C61} = \boldsymbol{a}_C \qquad (16)$$

For the acceleration at point C, the relation.

$$\boldsymbol{a}_{C51} = \boldsymbol{a}_{B51} + \boldsymbol{a}_{CB51} \qquad (17)$$

The acceleration at point B is completely known from relation (15) and therefore will not be decomposed into normal and tangential components. The other accelerations have to be found out. Relation (17), after decomposition into components, has the form.

$$\boldsymbol{a}_{C51} = \boldsymbol{a}_{B51n} + \boldsymbol{a}_{B51t} + \boldsymbol{a}_{CB51n} + \boldsymbol{a}_{CB51t} \qquad (18)$$

The magnitude of the normal components of the accelerations ($\boldsymbol{a}_{C51n}$ a $\boldsymbol{a}_{CB51n}$) can be determined using the Euclidean construction of the given accelerations; the magnitudes of the tangential components of the accelerations ($\boldsymbol{a}_{C51t}$ a $\boldsymbol{a}_{CB51t}$) are determined from the vector pattern.

The actual magnitudes of the given acceleration velocities obtained by the graphical solution are given in Table 1. The graphical solution has been carried out in a CAD program.

Table 1. Velocities and accelerations obtained by graphical solution

	point				
	A	BA	B	CB	C
a_n [ms^{-2}]	14.2122	1.2828	1.3956	0.9306	0.0668
a_t [ms^{-2}]	0	5.8632	13.0544	12.6994	2.6872
a [ms^{-2}]	14.2122	6.002	13.1286	12.7334	2.6882
v [ms^{-1}]	0.75398	0.7427	0.44984	0.42598	0.16946

3 Motion simulation of the mechanism

The program allows to perform kinematic and dynamic analyses of mechanical systems of points or bodies, both rigid and flexible, as well as analyses of the strength of structural elements, sensing of forces in motion with consideration of gravitational, inertial effects or frictional forces, etc. The software also offers the possibility to

Acta Mechatronica - International Scientific Journal about Mechatronics
Volume: 7 2022 Issue: 1 Pages: 1-7 ISSN 2453-7306

model a given mechanical system directly in its own environment using the CAD functions it offers, or this model of the mechanism, mechanical system can be imported from various CAD software (e.g. from software such as Inventor, SolidWorks and others) in .sat, .step, .iam and other formats [8-12].

3.1 Model creation

The simulation was performed in MSC.Adams/View [13,14]. In this program, the individual members of the mechanism were successively modelled according to the simplified scheme in Fig. 2. The modelling function "RigidBody:Link" was used to create the individual members. When modelling the crank, the rotation point O_2 is placed in the position (0, 0, 0) mm and the length is defined according to the given dimensions. The crank is rotated in a position 60° from the x-axis. This is done by rotating the end markers by an angle of (300, 0, 0, 0)°, due to the fact that the angle of rotation about the z-axis is measured counterclockwise from the x-axis in the program. The buckling plate (member 4) is positioned so that its rotation point O_4 is at the position (125, -435, 0) mm. The connecting rod is attached to the pre-existing crank 2. The jaw has a pivot point at point O_6 with coordinates (-150, 0, 0) mm. A second buckling plate (member 5) is attached to this jaw. A model of the crusher mechanism is shown in Fig. 3.

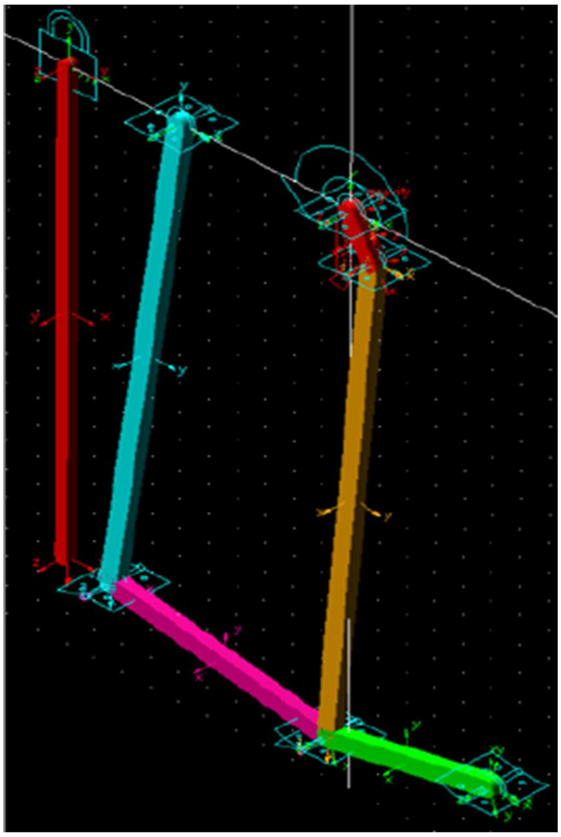

Figure 3 Kinematic model of the crusher mechanism

The individual members of the mechanism are connected by rotary linkages. After the model is assembled, the model is subjected to verification.

The driving member 2 (eccentric shaft) performs a rotary motion and rotates at an angular velocity of $\omega_2 = 6\pi\ rad/s$, which when converted to degrees per second is $\omega_2 = 1080\ °/s$. The crank makes 3 rotations in 1 second. The rotational motion is placed at the crank turning point O_2. The simulation is set so that the crank makes one revolution (360° rotation), and thus the simulation time is one-third of a second. The step size is set to 0.001.

In order to be able to obtain individual data of the monitored quantities during the movement of the mechanism, their meters were defined in the program, such as speed meter, acceleration meter, etc... In addition to the measurement of speed and acceleration, the angles of rotation of some members were also measured. The obtained results were processed in the postprocessor, in the form of graphs and tables.

3.2 Simulation results of selected variables

The simulation is run from an initial position where the driving member 2 is rotated by an angle $\varphi = 60°$ below the x-axis. This is in order to be able to compare the values obtained for the individual variables from the computer simulation with the values obtained by the graphical solution. The advantage of the simulation is that it offers the waveforms of the given quantities also depending on the movement of the driving member, i.e. during the action of the mechanism cycle.

Figure 4 shows the time history of the angle of the member 2. Figure 5 shows the waveform of the dependence of the angle of member 6 on the rotation of member 2 when the crank is turned one revolution. The angle of the movable jaw is measured from the x-axis.

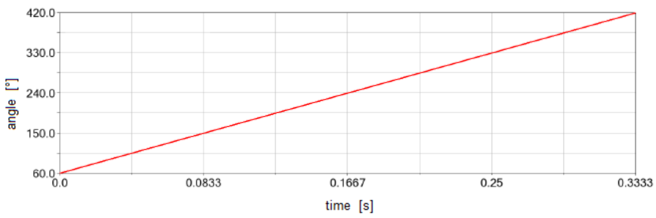

Figure 4 Time history of crank angle (member 2)

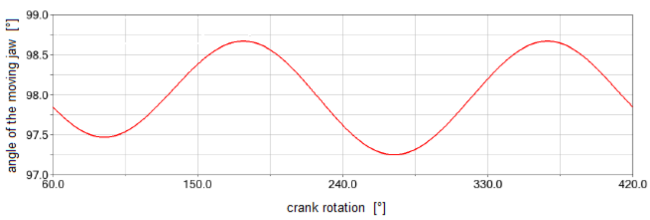

Figure 5 Course of the angle of the movable jaw (member 6) as a function of the rotation of the crank (member 2)

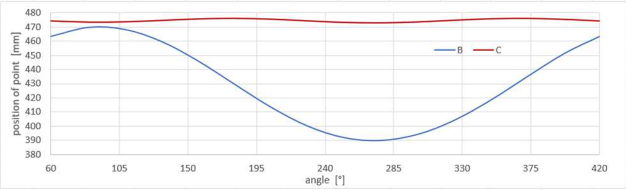

Figure 6 Dependence of the position of a point on the angle of rotation of the member 2

Figure 6 shows the dependence of the position of points B and C on the angle of rotation of the crank by one turn. From Figure 6, it can be seen that at one turn of the crank, the movable jaw approaches the fixed jaw twice. The first advancement of the movable jaw from the fixed jaw is less than the second advancement. The values at the moment when the movable jaw is closest to the fixed jaw are the same in both cases.

For the magnitude of the individual resulting accelerations at the given points, it is valid that they are equal to the square root of the sum of the squares of the components of the given acceleration.

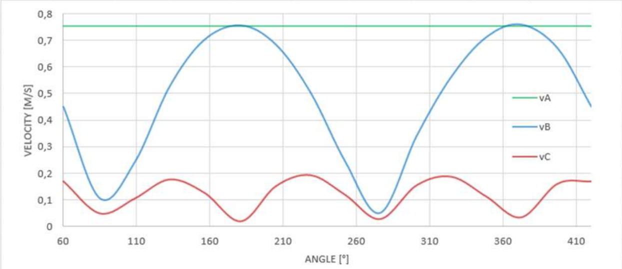

Figure 7 Velocity magnitude of single points as a function of member rotation angle 2

Figure 7 shows the evolution of the velocity of the individual points of the mechanism as a function of the angle of rotation of the crank when the crank is turned one revolution. Figure 8 shows the waveform of the acceleration components of point B as a function of the crank rotation. The resulting acceleration curves of the individual points of the mechanism as a function of crank rotation are shown in Figure 9.

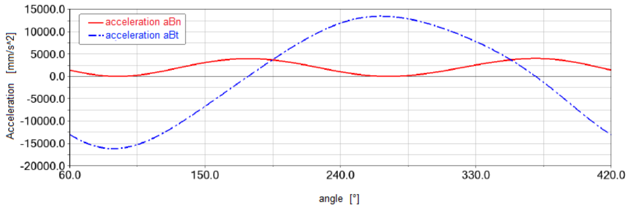

Figure 8 Acceleration components at point B as a function of crank rotation

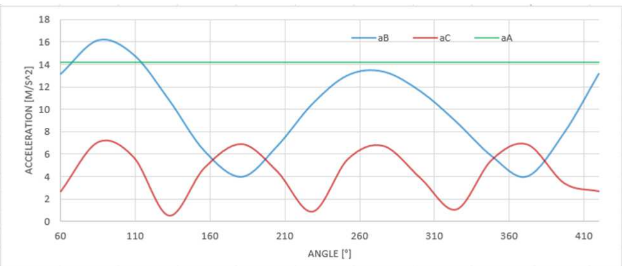

Figure 9 Acceleration of single points as a function of the angle of rotation of the member 2

3.3 *Point trajectory*

The advantage of the program and the simulation itself is that it can also provide a representation of the paths of given points. The trajectories of points A, B and C are shown using the "Trace Marker" function in Figure 10. The trajectory of point A is a circle, the trajectories of points B and C are circular arcs.

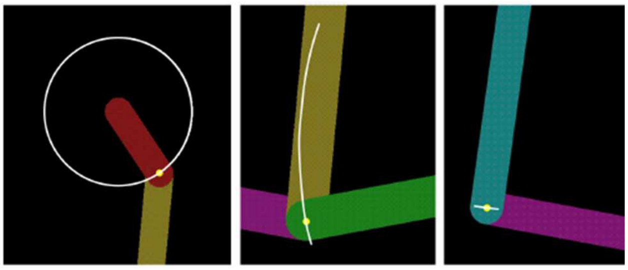

a) b) c)

Figure 10 Trajectory of (a) point A, (b) point B, (c) point C

Another way to plot the path or trajectory of a given point during the movement of the mechanism is to plot it in the postprocessor as the dependence of the x-axis position of the component point on the y-axis component of the y-axis position. The individual point trajectories are shown in Figure 11.

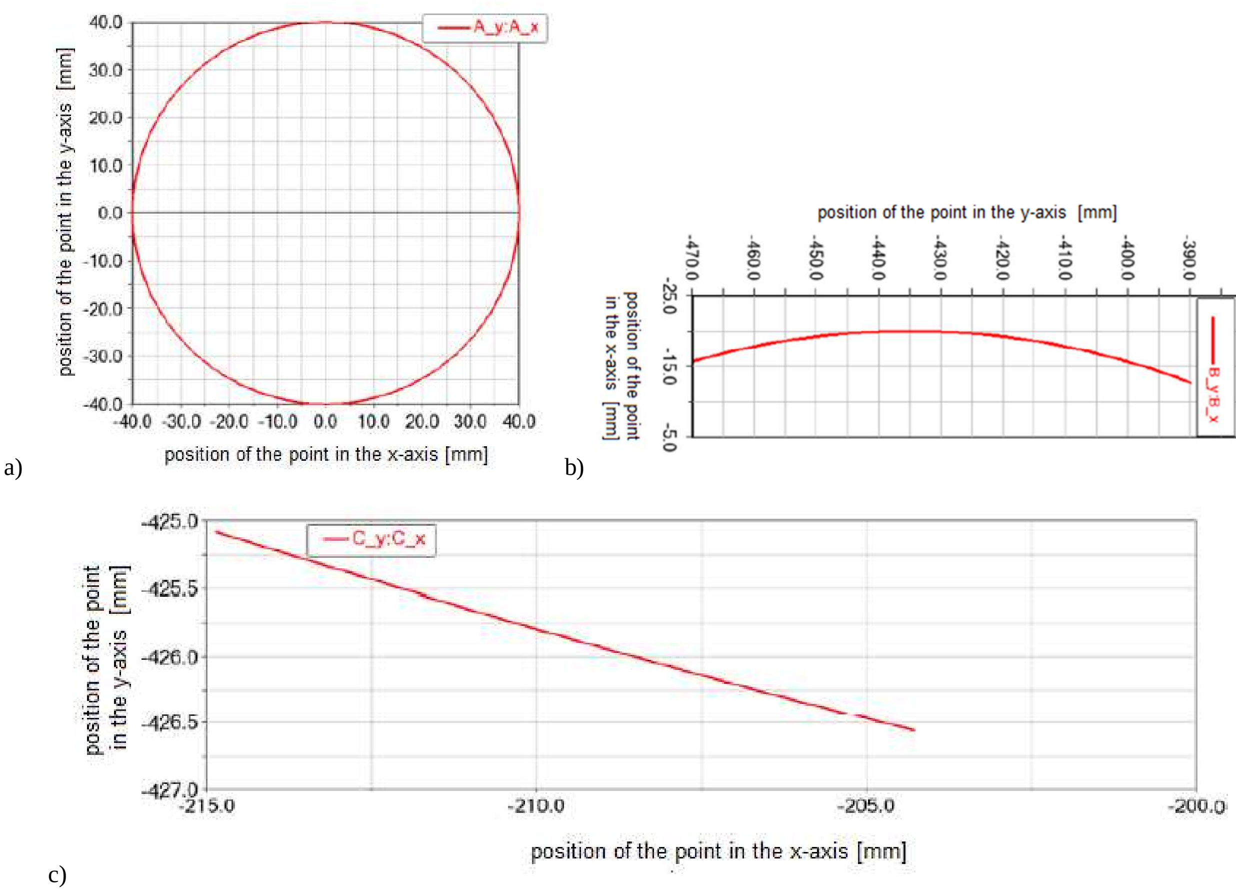

Figure 11 Trajectory of (a) point A, (b) point B, (c) point C

3.4 Comparison of results obtained by graphical solution and simulation

The displacements obtained by graphical solution and simulation were compared in the initial position of the mechanism. The individual deviations of the solutions are shown in Table 2. The largest differences in the results are visible only at the ten-thousandths place.

Table 2 Comparison of results obtained by graphical solution and simulation

	Graphic solution	Computer simulation	Difference
v_A [ms^{-1}]	0,75398	0,75398	0,00000
v_B [ms^{-1}]	0,44984	0,44984	0,00000
v_C [ms^{-1}]	0,16946	0,16946	0,00000
a_A [ms^{-2}]	14.21220	14.21223	0,00003
a_B [ms^{-2}]	13,12860	13,12876	0,00016
a_C [ms^{-2}]	2,68820	2,68813	-0,00007
a_{BA} [ms^{-2}]	6,00200	6,00200	0,00000
a_{CB} [ms^{-2}]	12,73340	12,73346	0,00006

4 Conclusion

In this paper, the kinematic analysis of the planar six-joint mechanism of a two-spring jaw crusher has been carried out. The kinematic analysis of the mechanism was solved graphically and by computer simulation.

The graphical solution was carried out using Autodesk Inventor Professional 2020 with the mechanism in the initial position. Kinematic analysis using computer simulation was solved using MSC.Adams/View program, where the waveforms and magnitudes of the given quantities during one complete cycle of the mechanism and the trajectories of the given points were obtained.

Based on the comparison of the results obtained by the two solution methods, it can be stated that the accuracy of the results obtained from the simulation is quite high compared to the graphical solution. One can speak of very small to imperceptible differences in the results, since the largest differences in the results found are in the order of 10^{-4} to 10^{-5} units.

Thus, the use of computer simulation of the mechanism is a suitable and advantageous choice for kinematic analysis, also because it provides results not only at a single instant, as in the graphical solution, but during the whole process or cycle. The given results can be processed in the form of graphs or even tables, and the simulation also provides an insight into how the mechanism will perform the prescribed motion.

Acknowledgements
This work was supported by the Ministry of Education of Slovakia Foundation under Grant project, VEGA No. 1/0436/22, VEGA No. 1/0500/20 and KEGA No. 027TUKE–4/2020.

[1] VAVRO jr, J., VAVRO, J., KOVÁČIKOVÁ, P., BEZDEDOVÁ, R., HÍREŠ, J.: Kinematic and dynamic analysis and distribution of stress in items of planar mechanisms by means of the MSC ADAMS software, *Manufacturing technology*, Vol. 17, No. 2, pp. 267-270, 2017.
[2] RATIU, M., RUS, A., BALAS, M.L.: *Modeling in ADAMS of a 6R industrial robot*, MATEC Web of Conferences, Vol. 184, pp. 1-4, 2018.
[3] HRONCOVÁ, D., DELYOVÁ, I., FRANKOVSKÝ, P.: *Kinematic analysis of mechanisms using MSC Adams*, Applied Mechanics and Materials, Trans Tech Publications Ltd, pp. 83-89, 2014.
[4] KOCHANOWSKY, B.: Portable crusher for open pit and quarry operations, *Transactions of the American Institute of Mining, Metallurgical Petroleum Engineers*, Vol. 220, pp. 271-274, 1961.
[5] BALASUBRAMANIAN, A.: Size reduction by crushing methods, ResearchGate, pp. 1-10, 2017. https://doi.org/10.13140/RG.2.2.28195.45606
[6] SAPIETOVÁ, A., DEKÝŠ, V.: Dynamic analysis of rotating machines in MSC ADAMS, *Procedia Engineering*, Vol. 136, pp. 143-149, 2016.
[7] BOCKO, J., DELYOVÁ, I., FRANKOVSKÝ, P.: *Kinematika*, Košice, 2012. (Original in Slovak)
[8] DELYOVÁ, I., HRONCOVÁ, D., FRANKOVSKÝ, P.: Analysis of simple mechanism using MSC Adams, *Manufacturing Technology*, Vol. 14, No. 2, pp. 141-145, 2014.
[9] HRONCOVÁ, D., DELYOVÁ, I.: Computer Simulation Using MSC ADAMS, *Acta Mechatronica*, Vol. 5, No. 3, pp. 41-46, 2020. https://doi.org/10.22306/am.v5i3.67
[10] SAPIETOVÁ, A., SÁGA, M., KURIC, I., VÁCLAV, Š.: Application of optimization algorithms for robot systems designing, *International journal of advanced robotic systems*, Vol. 15, No. 1, 2018.
[11] MAHMOOD, K., ISMAIL, N.A.: Application of multibody simulation tool for dynamical analysis of tethered aerostat, *Journal of King Saud University-Engineering Sciences*, Vol. 34, No. 3, pp. 209-216, 2020.
[12] ARMAN, R.: *Kinematic analysis on four-bar mechanism model using PID Controller*, The 5th Engineering Science & Technology International Conference, IOP Publishing, IOP Conf. Series: Materials Science and Engineering 990, 2020. 10.1088/1757-899X/990/1/012029
[13] HRONCOVÁ, D., FRANKOVSKÝ, P., VIRGALA, I., DELYOVÁ, I.: Kinematic Analysis of the Press Mechanism Using MSC Adams, *American journal of mechanical engineering*, Vol. 2, pp. 312-315, 2014.
[14] ZAR, T., LIN, P.W., WIN, S.Y.: Workspace Analysis of Two-link Planar Manipulator, *Int. J. of Science and Engineering Applications*, Vol. 8, pp. 380-383, 2019.

Review process
Single-blind peer review process.